Int. J. Exp. Path. (2008), 89, 81–90
doi: 10.1111/j.1365-2613.2007.00568.x

ORIGINAL ARTICLE

Cleavage and conformational changes of tau protein follow phosphorylation during Alzheimer's disease

Siddhartha Mondragón-Rodríguez*,[1], Gustavo Basurto-Islas*,[1], Ismael Santa-Maria[†], Raúl Mena[‡], Lester I. Binder[§], Jesús Avila[†], Mark A. Smith[¶], George Perry[¶,**] and Francisco García-Sierra*

*Departments of Cell Biology, CINVESTAV-IPN, México City, México, [†]Centro de Biología Molecular 'Severo Ochoa' (CSIC-UAM), Universidad Autónoma de Madrid, Cantoblanco, Madrid, Spain, [‡]Departments of Neuroscience, CINVESTAV-IPN, México City, México, [§]Department of Cell and Molecular Biology, Northwestern University Medical School, Chicago, IL, USA, [¶]Department of Pathology, Case Western Reserve University, Cleveland, OH, USA and **College of Sciences, University of Texas at San Antonio, San Antonio, TX, USA

INTERNATIONAL JOURNAL OF EXPERIMENTAL PATHOLOGY

Summary

Phosphorylation, cleavage and conformational changes in tau protein all play pivotal roles during Alzheimer's disease (AD). In an effort to determine the chronological sequence of these changes, in this study, using confocal microscopy, we compared phosphorylation at several sites ($Ser^{199/202/396/404/422}$-$Thr^{205}$ and the second repeat domain), cleavage of tau (D^{421}) and the canonical conformational Alz-50 epitope. While all of these posttranslational modifications are found in neurofibrillary tangles (NFTs) at all stages of the disease, we found significantly higher numbers of phospho-tau positive NFTs when compared with cleaved tau ($P = 0.006$ in Braak III; $P = 0.002$ in Braak IV; $P = 0.012$ in Braak V) or compared with the Alz-50 epitope ($P < 0.05$). Consistent with these findings, in a double transgenic mice model (Tet/GSK-3β/VLW) overexpressing the enzyme glycogen synthase kinase-3β (GSK-3β) and tau with a triple FTDP-17 mutation (VLW) with AD-like neurodegeneration, phosphorylation at sites $Ser^{199/202}$-Thr^{205} was greater than truncated tau. Taken together, these data strongly support the notion that the conformational changes and truncation of tau occur after the phosphorylation of tau. We propose two probable pathways for the pathological processing of tau protein during AD, either phosphorylation and cleavage of tau followed by the Alz-50 conformational change or phosphorylation followed by the conformational change and cleavage as the last step.

Received for publication:
17 September 2007
Accepted for publication:
17 October 2007

Correspondence:
Dr Francisco Garcia-Sierra
Department of Cell Biology
Center of Research and Advanced Studies of the National Polytechnic Institute
Av. Instituto Politecnico Nacional 2508, CP 07360
Mexico City
Mexico
Tel.: +52 555 061 33 54
Fax: +52 555 061 33 93
E-mail: fgarcia-sierra@cell.cinvestav.mx

[1]S. M.-R. and G. B.-I. contributed equally to this work

Keywords
Alzheimer's disease, tau cleavage, tau conformation, tau phosphorylation

In Alzheimer disease (AD), an important role for tau protein is well-documented (Iqbal *et al.* 1998; King *et al.* 1999; Gamblin *et al.* 2000; Avila *et al.* 2004; Binder *et al.* 2005) with neurofibrillary tangles (NFTs) composed of highly phosphorylated forms of tau accumulating in the hippocampus and correlating to dementia (Van Hoesen & Hyman 1990; Van Hoesen *et al.* 1991; Baumann *et al.* 1993; Bramblett *et al.* 1993; Alonso *et al.* 1996, 2001). In addition to the well known changes in phosphorylation state, tau also undergoes multiple truncation and conformational changes that likely occur in an orderly pattern (Carmel *et al.* 1996; Garcia-Sierra *et al.* 2001, 2003; Ghoshal *et al.* 2001; Gamblin *et al.* 2003a,b; Binder *et al.* 2005; Guillozet-Bongaarts *et al.* 2005; Luna-Munoz *et al.* 2005). Nonetheless, an accurate spatial pattern of the appearance of each pathological event remains to be further investigated.

One of the major physiological roles for tau involves microtubule dynamics and stabilization. Additionally, tau is also proposed to be involved in signal transduction, organelle transport and cell growth (Timm *et al.* 2006; Yu & Rasenick 2006; Bullmann *et al.* 2007). The C-terminal region of tau plays an important role in binding to microtubules (Timm *et al.* 2006; Yu & Rasenick 2006; Bullmann *et al.* 2007), which is regulated by phosphorylation and dephosphorylation of the repeat domain and other regions (Gustke *et al.* 1994; Goode *et al.* 1997).

In AD, tau is highly phosphorylated at several sites, including those recognized by AT8 and PHF-1 antibodies, and while this phosphorylation results in reduced binding to microtubules *in vitro*, the effect *in vivo* is less clear (Otvos *et al.* 1994; Goedert *et al.* 1995; Cash *et al.* 2003).

In AD, cell loss is another major characteristic and enzymes involved in apoptosis, such as cysteine aspartate proteases, including activated caspases (caspases 3, 6, 8 and 9), are increased in hippocampal and temporal cortical neurons in AD brains (Raina *et al.* 2001; Rohn *et al.* 2001, 2002; Matsui *et al.* 2006). While it is likely that these proteases contribute to neurodegeneration, whether this relates to bona fide apoptosis remains obscure (Raina *et al.* 2001, 2003; Rohn *et al.* 2001, 2002; Zhu *et al.* 2004, 2006). On the other hand, the role of caspase-3 in the cleavage of tau at D^{421} is irrefutable (Gamblin *et al.* 2003b; Rissman *et al.* 2004).

As discussed above, while the phosphorylation, conformational changes and cleavage of tau protein are important events that lead to the pathological state of tau protein observed during AD, the chronology of these changes is still under investigation. Very recently it was demonstrated in AD brains that phosphorylation precedes truncation during NFTs maturation, particularly the phospho-S^{422} residue occurring early than the cleavage at D^{421} (Guillozet-Bongaarts *et al.* 2006). To further analyse this, in the present study we used double and triple labelling laser scanning confocal microscopy to determine the spatial and temporal relationship of phosphorylation, conformational changes, and cleavage of tau protein during AD pathology. We selected a population of cases displaying characteristic neurofibrillary degeneration according to Braak stages II–V. Our findings show a well-defined pathway with phosphorylation as the earliest event when compared with other pathological events such as cleavage at site D^{421} and the canonical Alz-50 conformational change.

Material and methods

Brain tissue

Brain tissue was obtained from a population-based sample of elderly cases in the city of Cambridge (UK). Clinical diagnosis of AD was made using CAMDEX (Roth *et al.* 1986). Cases included AD and control age-matched normal individuals. From the entire population, we randomly selected cases with progressive neurofibrillary degeneration according to Braak stages II–V, [BST II: four cases; BST III: six cases; BST IV: four cases; BST V: six cases, (Braak & Braak 1991; Braak *et al.* 1994)]. We excluded Braak stages I and VI from this morphometric study because of their relatively small sample size.

The brains were obtained postmortem and cut in the sagittal plane. Half was frozen at −70 °C, while the other half of the brain was fixed in buffered 10% formalin for 3 weeks. The paraffin-embedded blocks were cut into 10-μm thick sections and used for immunostaining and morphometry.

Double and triple labelling immunofluorescence

After rehydration (fixed tissue) through xylene and graded ethanols, sections were blocked with 10% normal goat serum (Sigma, St. Louis, MO, USA) in Tris-buffered saline (TBS, 50 mM Tris, 150 mM NaCl pH 7.6) for 30 min. Double and triple labelling experiments were conducted using combinations of the antibodies listed in Table 1. IgG and IgM primary mouse monoclonal antibodies were detected with FITC, TRITC or Cy5 conjugated goat anti-mouse IgG (γ-specific) and FITC or TRITC anti-mouse IgM (μ-specific) (Jackson Immuno Research Laboratories, Bar Harbor, ME, USA) as secondary antibodies. For experiments using a rabbit primary polyclonal, anti-rabbit IgG secondary antibodies were used (Jackson Immuno Research Laboratories, Bor Harbor, ME, USA). Adjacent serial sections were used to directly compare pathological structures

recognized by different antibodies. In all the experiments, incubation with primary antibodies was overnight at 4 °C, followed by 1 h at room temperature with corresponding secondary antibodies. The sections were mounted in antiquenching medium (Vectashield; Vector Laboratories, Inc. Burlingame, CA, USA).

Some sections were also labelled with tiazin red (TR) to localize pathological β-sheet structures.

Immunohistochemistry

After deparaffinization and rehydration, sections were incubated for 15 min with 0.3% hydrogen peroxide in phosphate-buffered saline (PBS), pH 7.4, to inactivate endogenous peroxidases. The monoclonal antibodies Tau-C3 and AT8 (on adjacent serial sections), were incubated overnight at 4 °C. Horseradish peroxidase (HRP) secondary antibodies were respectively used, and the enzymatic reaction was developed by incubation with 0.01% hydrogen peroxide in PBS (pH 7.4) containing 0.06% diaminobenzidine. The reaction was stopped and sections dehydrated and mounted in DPX.

Confocal microscopy

Labelled brain sections were viewed with a 40× oil immersion Plan-Apochromat on a TCP-SP2 Leica (Heidelberg, Germany) laser scanning-confocal microscope. Additional high power lenses (60× and 100×) were used to critically evaluate co-localization in single optical sections. Confocal images were obtained as single sections and the stack of images was projected as individual 2D extended focus images. Resulting images were analysed using the software included with the microscope.

Statistical Analyses and Morphometry

Using the peroxidase technique, NFTs were counted in the hippocampal area. Per case, morphometric quantification in the areas was assessed on three microscopic fields from randomly chosen regions in the area of interest. Observations were conducted by bright field microscopy (eclipse 80i; Nikon Inc., Melville, NY, USA). Identification and counting of pathological structures was conducted using 20× and 40× objective lenses and values expressed per square millimetre as previously described (Garcia-Sierra *et al.* 2001).

Student's *t*-test was applied when NFTs counts were compared between different antibodies (Figures 2 and 5). Statistical analysis was conducted with SPSS for Windows 10.0 version (SPSS Inc., Chicago, IL, USA) and GraphPad Prism software 3.0 version (GraphPad Software Inc., San Diego, CA, USA).

Transgenic mice

Using the tet-regulated system (Gingrich & Roder 1998), a double transgenic mice model (Tet/GSK-3β/VLW) was previously generated (Engel *et al.* 2006c) and used here. For this purpose, the transgenic model overexpressing the enzyme glycogen synthase kinase-3β (GSK-3β) (Tet/GSK-3β mice) was combined with transgenic mice expressing tau with a triple frontotemporal dementia and parkinsonism linked to chromosome 17 (FTDP-17) mutation which develop prefibrillar tau-aggregates (VLW mice) (Engel *et al.* 2006a–c).

Results

Phosphorylation at sites Ser$^{199/202}$-Thr^{205} and cleavage at site D^{421} are hallmarks of Alzheimer's disease

Single-labelled immunohistochemistry in AD cases representative of several Braak stages was performed using AT8 (phosphorylation at sites Ser$^{199/202}$-Thr^{205}) and Tau-C3 (cleavage tau at D^{421}) antibodies. We found the well described NFTs pathology within the hippocampal area contained tau phosphorylation at sites Ser$^{199/202}$-Thr^{205} (Figure 1d–f). We also found substantial NFTs pathology with truncated tau at D^{421} (Figure 1a–c) in the same area. As shown in Figure 1c,f, there were quantitative differences with greater numbers of NFTs-containing phosphorylation at those sites than cleavage at site D^{421}.

Significantly higher numbers of AT8 immunoreactive NFTs were found in AD brains from Braak stages III to V

To further analyse if phosphorylation at Ser$^{199/202}$-Thr^{205} is an event that precedes cleavage at D^{421}, we analysed cases with progressive neurofibrillary pathology [stages II–V (Braak & Braak 1991; Braak *et al.* 1994)]. Neurofibrillary tangles were counted in adjacent CA1 hippocampal areas using AT8 and Tau-C3. In all cases, including Braak III–V, the density of intracellular tangles containing phosphorylated tau at sites Ser$^{199/202}$-Thr^{205} was significantly higher when compared with cleavage at D^{421} ($P = 0.006$ in Braak III; $P = 0.002$ in Braak IV; $P = 0.012$ in Braak V respectively, Figure 2). In those cases from Braak II, no significant difference was found between AT8 and Tau-C3 immunolabelled NFTs, however, at this stage the CA1 area demonstrated a large amount of pretangle cells displaying AT8

Table 1 Antibodies employed

State	Antibody	Class	Epitope	Reference
Phosphorylation dependent	AT8	IgG	$pSer^{202}$, $pThr^{205}$	Goedert *et al.* (1995)
	pTau	IgG	Second repeat domain	ABR, Inc. Golden, CO 80401, USA.
	Ser^{396}	IgG	$pSer^{396}$	Bramblett *et al.* (1993)
	Ser^{422}	IgG	$pSer^{422}$	Biosource, Camarillo, CA, USA.
Conformation dependent	Alz-50	IgM	5–15; 312–322	Carmel *et al.* (1996)
Truncation dependent	Tau-C3	IgG	Truncation D^{421}	Gamblin *et al.* (2003b)

staining with no fibrillar appearance. Moreover, neuritic component immunoreactive to AT8 antibody was also predominant along the neuropil of CA1 area. These results suggest that phosphorylation of tau in assembled and non-assembled conformation precedes D^{421} truncation. No pretangles stages were decorated by Tau-C3 antibody (data not shown).

These data support the hypothesis of phosphorylation as an earlier pathological feature than the truncation at site D^{421} in tau protein during AD pathology at early stages.

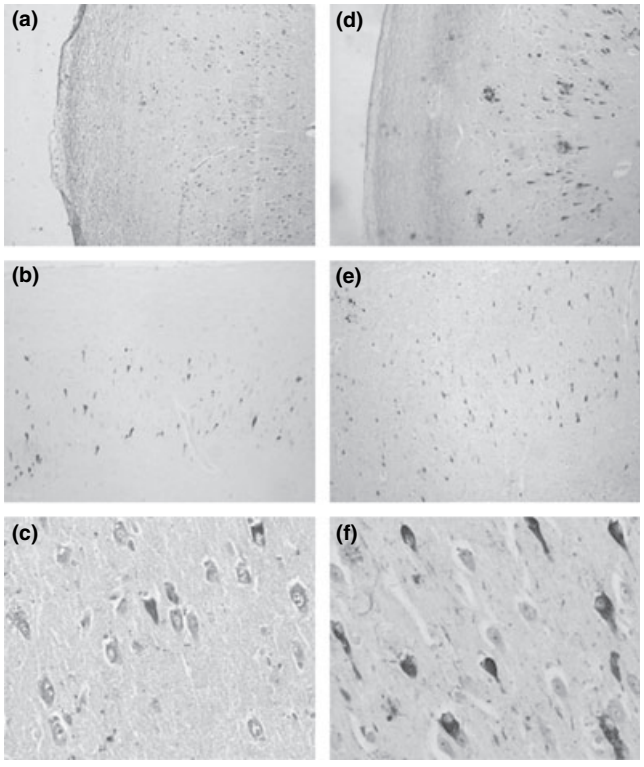

Figure 1 Immunohistochemistry of tau protein in the hippocampal area of AD cases demonstrating that Tau-C3 reacts with the canonical neurofibrillary tangles (NFTs) (a–c) as well as AT8 (d–f). Identification of structures was conducted using 20× (a, b, d and e) and 40× (c and f) objective lenses.

Phosphorylation at sites Ser^{199}, second repeat domain (pTau) and Ser^{422} are coincident with cleaved tau protein at D^{421}

The pattern of phosphorylation at Ser^{199} and cleavage at D^{421} was examined in the hippocampus in several AD cases. We observed that both events (phosphorylation at Ser^{199} and cleavage at D^{421}) were coincident in the NFTs pathology (Figure 3a). When we analysed the phosphorylation at the second repeat domain (pTau) we saw a similar pattern, the phosphorylation in the second repeat domain and cleaved tau at D^{421} were always coincident (Figure 3b). Interestingly, in no case were NFTs present with the opposite pattern, i.e. no structures present with truncation but no phosphorylation at Ser^{199} or the second repeat domain (see Discussion).

Tau phosphorylated at Ser^{422} was observed co-labelled with hippocampal NFTs pathology (Figure 3d). Interestingly, here immunostaining patterns emerged, NFT pathology with

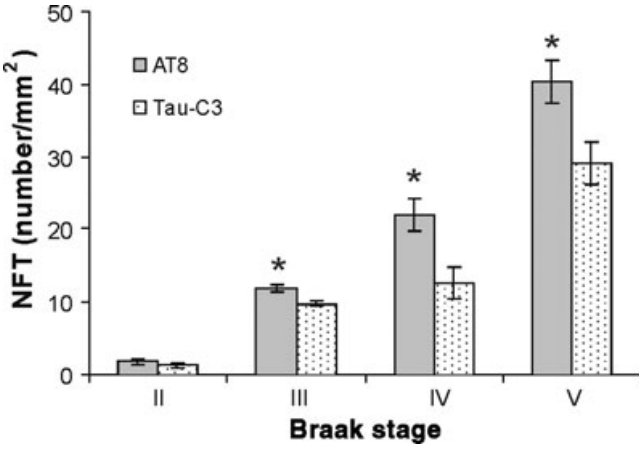

Figure 2 Significantly higher numbers of phosphorylation at sites $Ser^{199/202}$-Thr^{205} (AT8) immunoreactive NFTs were found in Alzheimer's disease (AD) brains corresponding to Braak's staging III–V. Paraffin embedded brain sections from CPLL cases were studied by inmunohistochemistry with Tau-C3 (cleavage at site D^{421}) and AT8 and analysed under bright field. Significant differences (*) between the density of neurofibrillary tangles (NFTs) with AT8 and Tau-C3 were found ($P = 0.006$ in Braak III; $P = 0.002$ in Braak IV; $P = 0.012$ in Braak V respectively).

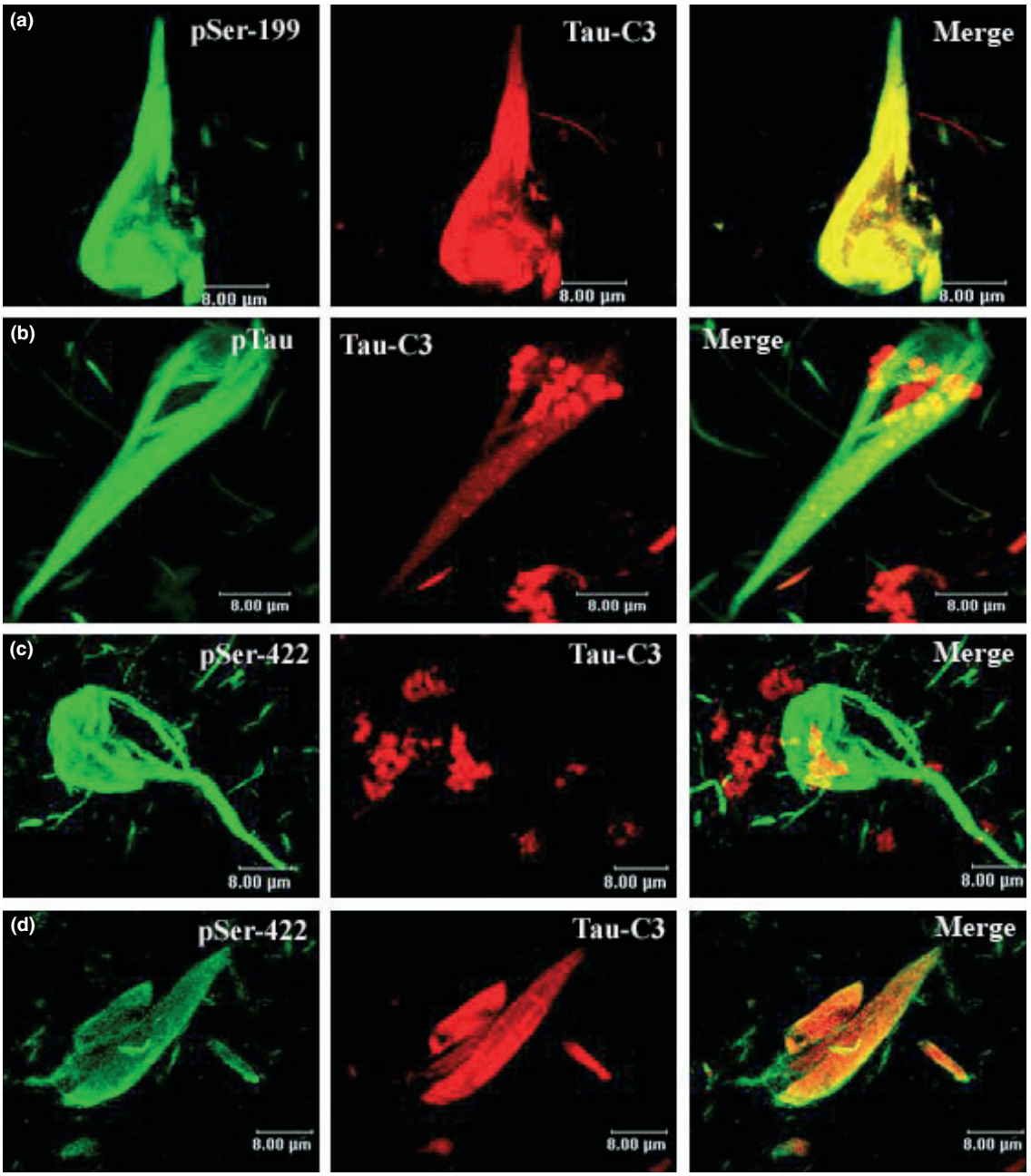

Figure 3 Confocal microscopic images demonstrating that cleavage at D^{421} and phosphorylation colocalize in Alzheimer's disease (AD) brain. Double immunofluorescence was used to examine the association of cleavage at D^{421} (red) and the phosphorylation at several sites (green). The cleavage of tau at D^{421} was coincident with the phosphorylation at sites Ser^{199} (a), Ser^{422} (d) and the second repeat domain labelled by pTau (b). Truncation at D^{421} (red) was coincident with phosphorylation at Ser^{422} (green) in the latest structures (d), but in the youngest, we did not found tau truncated protein at D^{421} associated with this phosphorylation (c).

both events (phosphorylation at site D^{422} and cleavage at site D^{421}) and NFTs with just phosphorylation at site Ser^{422} (Figure 3c,d).

In sum, tau protein cleavage at D^{421} was coincident with phosphorylation at sites Ser^{199}, second repeat domain, and Ser^{422} sites in early stages of NFTs development.

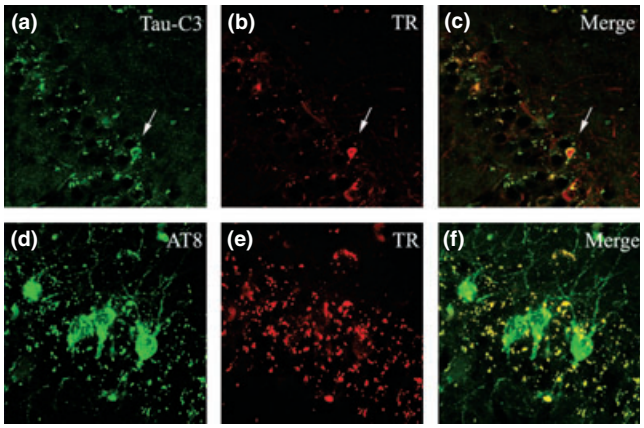

Figure 4 Neurofibrillary tangle (NFTs) pathology in CA1 formation from the hippocampal area mainly composed by phosphorylated tau at sites $Ser^{199/202}$-Thr^{205} was found in transgenic mice (green NFTs, d). Lack of β-sheet conformation as assessed by tiazin red (TR) staining in the AT8 pathology was observed (e, f). Neurofibrillary tangle pathology composed by truncated tau at site D^{421} was also found in the same area (white arrow, a). Identification of structures was conducted using 20× (a–c) and 40× (d–f) objective lenses.

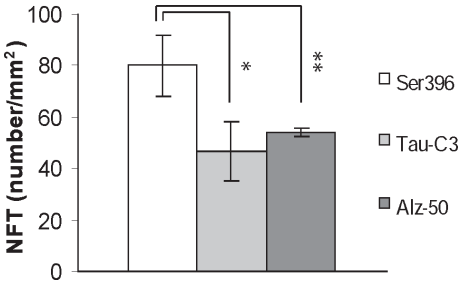

Figure 5 Significantly higher numbers of phosphorylation at sites Ser^{396} immunoreactive neurofibrillary tangles (NFTs) were found in Alzheimer's disease (AD) brains. Phosphorylation at site Ser^{396} is significantly increased when compared with cleavage at site D^{421} and significantly increased when compared with the conformational Alz-50 epitope (for both comparisons: $P < 0.05$).

NFTs containing hyperphophorylated tau were increased when compared with NFTs containing truncated tau in GSK-3β conditional transgenic mice

Using a double transgenic mice (Tet/GSK-3β/VLW) AD-like neurodegeneration model (Engel *et al.* 2006c), we analysed whether the chronology of phosphorylation at sites $Ser^{199/202}$-Thr^{205} labelled by AT8 and the cleavage of tau at site D^{421} labelled by TauC3 followed what was observed in AD. Tiazin red (TR) was used to identify β-sheet conformation. In the CA1 formation of the hippocampal

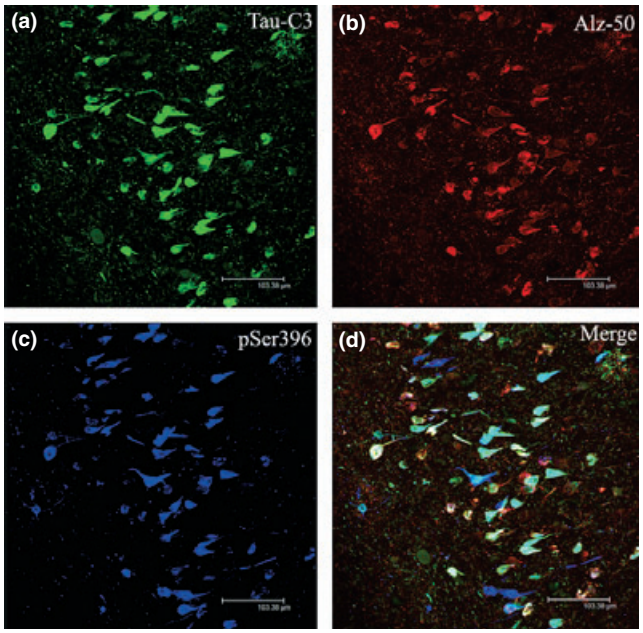

Figure 6 Confocal microscopic images demonstrating that cleavage at D^{421}, phosphorylation and the conformational Alz-50 epitope colocalize in Alzheimer's disease (AD) brain. Triple labelling immunofluorescence with Tau C3, Alz-50 and $pSer^{396}$. Neurofibrillary tangles (NFTs) with truncated tau at D^{421} and phosphorylation at Ser^{396} were found (white–blue NFTs, d); as well as NFT with phosphorylation at site Ser^{396}, cleavaged at site D^{421} and the Alz-50 conformational change (white NFTs, d); and finally NFTs with nothing but phosphorylation at site Ser^{396} (blue NFTs, Figure 4d).

area we found considerable NFTs pathology containing phosphorylated tau at sites $Ser^{199/202}$-Thr^{205} (green NFTs, Figure 4d). Interestingly, we observed a lack of β-sheet conformation as assessed by TR staining in the AT8 pathology (Figure 4e,f). Neurofibrillary tangle pathology containing truncated tau at site D^{421} was also found in the same area (white arrow, Figure 4a), although it was markedly reduced in comparison to the pathology labelled by AT8. As expected, the TauC3 pathology showed the typical β-sheet conformation as assessed by TR staining (white arrow, Figure 4b,c).

In AD, phosphorylation at sites Ser^{396}, cleavage of tau at D^{421} and the canonical Alz-50 epitope were found coincident during the NFT pathology

We found that phosphorylation at site Ser^{396} is increased when compared with cleavage at site D^{421} and also increased when compared with the conformational Alz-50 epitope (Figure 5).

Phosphorylation at Ser^{396} (blue colour, Figure 6c) and cleavage at site D^{421} (green colour, Figure 6a) were coincident in NFTs pathology (white and light blue colour, Figure 6d), similar to what we found when comparing truncated tau at D^{421} with phosphorylation at Ser^{199} and the second repeat domain (see results above). The phosphorylation at site Ser^{396} was also observed co-labelled with the canonical Alz-50 epitope (white colour, Figure 6d). Interestingly, some NFTs pathology display phosphorylation at Ser^{396} without the Alz-50 conformational change (blue NFTs, Figure 6d). On the other hand, the Alz-50 conformational change is mostly found co-localized with cleaved tau at D^{421}, while some truncated tau at this site (D^{421}) was found in the NFTs pathology without the Alz-50 conformational change (light blue NFTs, Figure 6d).

We also observed a population of NFTs that had all the events, phosphorylation at site Ser^{396}, the Alz-50 conformational change and the cleavage at site D^{421} (white colour NFTs, Figure 6d), suggesting a close and complicated relationship between all those events.

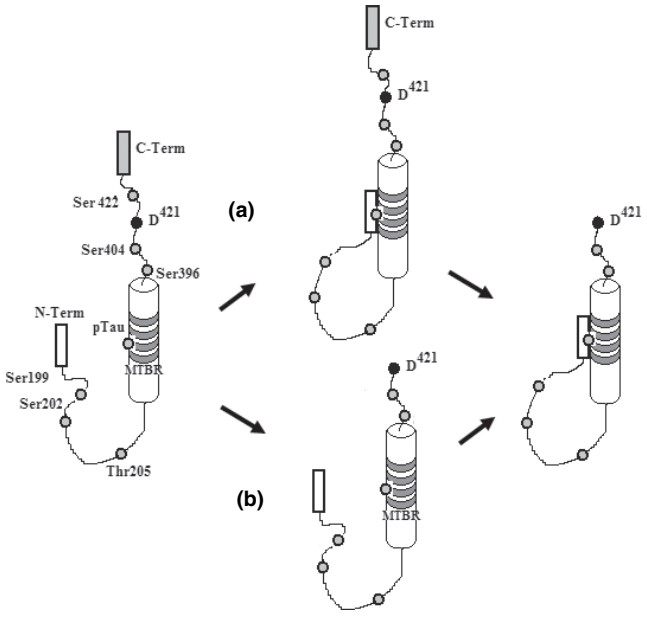

Figure 7 Maturation of Neurofibrillary tangles during Alzheimer's disease (AD) pathology follows a well defined pattern of phosphorylation in several sites such as $Ser^{199, 202, 396, 404, 422}$, Thr^{205} and second repeat domain, followed by cleavage of tau at D^{421} during early stages. According to our data, the pathological process of tau protein during AD could follow two pathways; (a) phosphorylation, conformational change and cleavage, or (b) phosphorylation, cleavage and conformational change.

Overall, in the hippocampal area of the AD cases, three populations of NFTs were found: (1) NFTs with only phosphorylation at site Ser^{396} (blue NFTs, Figure 6d); (2) NFT with truncated tau at D^{421} and phosphorylation at Ser^{396} (white–blue NFTs, Figure 6d); and (3) NFTs with phosphorylation at site Ser^{396}, cleavage at site D^{421} and the Alz-50 conformational change (white NFTs, Figure 6d).

Discussion

The phosphorylation, cleavage, and conformational changes of tau protein seem to play critical roles during AD pathology (Grundke-Iqbal *et al.* 1986; Bramblett *et al.* 1993; Alonso *et al.* 1996, 2001; Mena *et al.* 1996; Garcia-Sierra *et al.* 2001; Gamblin *et al.* 2003b; Gong *et al.* 2004; Luna-Munoz *et al.* 2005). Here, using specific antibodies to phsophorylation at $Ser^{199/202}$-Thr^{205} (AT8) and cleavage at D^{421} (Tau-C3), we found the typical NFTs pathology within the hippocampal area (Figure 1). To understand the spatial relationship of phosphorylation and cleavage at site D^{421} we used AD and control cases of varying pathological stages (Braak II–V) and found significantly higher numbers of AT8 immunoreactive NFTs compared with cleaved tau in most of the stages. Of note, at Braak II, NFTs composed of phosphorylated tau, while not significant, were more predominant than those composed of D^{421} truncated tau (Figure 2). Significantly, however, at this stage, large numbers of AT8-positive non-fibrillar pretangles are also detected, as well as a prominent neuritic component. This non-fibrillar pathology was not quantified in the present study but may be a previous step that contributes to NFTs formation. Tau-C3 immunoreactivity, on the other hand, was exclusive to NFTs and scarce labelling of neuritic component was evidenced at this stage (not shown). These data suggest that phosphorylation may function as an initiator, while cleavage could act as propagator during AD pathology.

To further analyse the spatial relationship of phosphorylation and cleavage during AD pathology, we performed double and triple confocal microscopy. A strong colocalization was observed between phosphorylation at Ser^{199} and the second repeat domain with cleaved tau in early NFTs (Figure 3a,b). The opposite pattern was never found, i.e. cleaved tau without phosphorylated tau. We also compared the phosphorylation at site Ser^{422} *vs.* the cleavage of tau at D^{421}. We found two patterns, phosphorylation at site Ser^{422} coincident with cleavage at D^{421} and phosphorylation at the same site without cleavage at D^{421} (Figure 3c,d). Similar to previous findings (Guillozet-Bongaarts *et al.* 2006), our data suggest that phosphorylation takes place

prior to the cleavage of tau at D^{421} and, as the phosphorylated epitope remains after the cleavage of tau, those NFTs are composed of different kinds of tau protein at different stages. These patterns also showed a dependent correlation between phosphorylation at several sites and cleavage at D^{421}. While little is known about downstream intracellular phosphorylation pathways, the activation of GSK-3β has been postulated to mediate AD tau hyperphosphorylation (Lucas *et al.*, 1993). Here, using a double transgenic mice (Tet/GSK-3β/VLW) AD-like neurodegeneration model (Engel *et al.* 2006c), we observed a similar chronological pattern between phosphorylation and cleavage. The phosphorylation at $Ser^{199/202}$-Thr^{205} was increased when compared with cleavage at D^{421} (Figure 4a,d). Interestingly, the phosphorylated NFTs were TR negative (Figure 4e), showing a lack of β-sheet structure, while the truncated NFTs were TR positive (Figure 4b, white arrow). These data suggest that phosphorylation is an event that takes place even when the tau protein is not fully processed as the β-sheet structure is not present.

At this point, our data suggest a well-defined pattern of cleaved tau at D^{421} preceded by phosphorylation at several sites. We also found that phosphorylation at Ser^{396} take place before the canonical Alz-50 epitope as well as the cleavage, as higher numbers of NFTs containing phosphorylation at Ser^{396} were observed when compared with the cleavage at site D^{421} and the Alz-50 conformational change (Figure 5). The Alz-50 conformational change, phosphorylation, and cleavage of tau were found coexisting in the same NFTs (Figure 6d), suggesting a close and complicated relationship between all those events during the pathological process. We also observed NFTs with nothing but phosphorylation, situating phosphorylation as the earliest event (Figure 6d) and directly contradicting earlier chronological schemas (Rissman *et al.* 2004). Interestingly, we found NFTs with phosphorylation and cleavage at D^{421} without the Alz-50 conformational change. These data suggest that phosphorylation takes place before the Alz-50 conformational change and the cleavage.

In conclusion, in this study, we show that phosphorylation and cleavage of tau are related during AD pathology, and both are early events that have a well-defined pattern of phosphorylation followed by cleavage. Our data also shows that phosphorylation is a major event during the early stages of AD pathology when compared with cleavage or the Alz-50 conformational change. Taken together, our analysis suggests that the tau processing during AD is taking two possible pathways: cleavage before Alz-50 conformational change, and vice versa, conformational change before cleavage (Figure 7).

Acknowledgements

We thank to Sandra Siedlak for the critical discussion and Dr Peter Davies for the use of Alz-50 antibody. This work was supported with grants from the CONACyT-Mexico to F.G-S (41023-M), and R.M (47630-M), and grants from the National Institutes of Health (AG026151 to M.A.S.) and Philip Morris USA, Inc. and Philip Morris International (to M.A.S. and G.P.). S.M-R was awarded with an international scholarship support from CONACyT-Mexico (200300).

References

Alonso A.C., Grundke-Iqbal I., Iqbal K. (1996) Alzheimer's disease hyperphosphorylated tau sequesters normal tau into tangles of filaments and disassembles microtubules. *Nat. Med.* **2**, 783–787.

Alonso A., Zaidi T., Novak M., Grundke-Iqbal I., Iqbal K. (2001) Hyperphosphorylation induces self-assembly of tau into tangles of paired helical filaments/straight filaments. *Proc. Natl Acad. Sci. USA* **98**, 6923–6928.

Avila J., Perez M., Lim F., Gomez-Ramos A., Hernandez F., Lucas J.J. (2004) Tau in neurodegenerative diseases: tau phosphorylation and assembly. *Neurotox. Res.* **6**, 477–482.

Baumann K., Mandelkow E.M., Biernat J., Piwnica-Worms H., Mandelkow E. (1993) Abnormal Alzheimer-like phosphorylation of tau-protein by cyclin-dependent kinases cdk2 and cdk5. *FEBS Lett.* **336**, 417–424.

Binder L.I., Guillozet-Bongaarts A.L., Garcia-Sierra F., Berry R.W. (2005) Tau, tangles, and Alzheimer's disease. *Biochim. Biophys. Acta* **1739**, 216–223.

Braak H. & Braak E. (1991) Neuropathological stageing of Alzheimer-related changes. *Acta Neuropathol. (Berl).* **82**, 239–259.

Braak E., Braak H., Mandelkow E.M. (1994) A sequence of cytoskeleton changes related to the formation of neurofibrillary tangles and neuropil threads. *Acta Neuropathol. (Berl).* **87**, 554–567.

Bramblett G.T., Goedert M., Jakes R., Merrick S.E., Trojanowski J.Q., Lee V.M. (1993) Abnormal tau phosphorylation at Ser396 in Alzheimer's disease recapitulates development and contributes to reduced microtubule binding. *Neuron* **10**, 1089–1099.

Bullmann T., de Silva R., Holzer M., Mori H., Arendt T. (2007) Expression of embryonic tau protein isoforms persist during adult neurogenesis in the hippocampus. *Hippocampus* **17**, 98–102.

Carmel G., Mager E.M., Binder L.I., Kuret J. (1996) The structural basis of monoclonal antibody Alz50's selectivity for Alzheimer's disease pathology. *J. Biol. Chem.* **271**, 32789–32795.

Cash A.D., Aliev G., Siedlak S.L. *et al.* (2003) Microtubule reduction in Alzheimer's disease and aging is independent of tau filament formation. *Am. J. Pathol.* **162**, 1623–1627.

Engel T., Goni-Oliver P., Lucas J.J., Avila J., Hernandez F. (2006a) Chronic lithium administration to FTDP-17 tau and GSK-3beta overexpressing mice prevents tau hyperphosphorylation and neurofibrillary tangle formation, but pre-formed neurofibrillary tangles do not revert. *J. Neurochem.* **99**, 1445–1455.

Engel T., Hernandez F., Avila J., Lucas J.J. (2006b) Full reversal of Alzheimer's disease-like phenotype in a mouse model with conditional overexpression of glycogen synthase kinase-3. *J. Neurosci.* **26**, 5083–5090.

Engel T., Lucas J.J., Gomez-Ramos P., Moran M.A., Avila J., Hernandez F. (2006c) Cooexpression of FTDP-17 tau and GSK-3beta in transgenic mice induce tau polymerization and neurodegeneration. *Neurobiol. Aging* **27**, 1258–1268.

Gamblin T.C., King M.E., Dawson H. *et al.* (2000) In vitro polymerization of tau protein monitored by laser light scattering: method and application to the study of FTDP-17 mutants. *Biochemistry (Mosc).* **39**, 6136–6144.

Gamblin T.C., Berry R.W., Binder L.I. (2003a) Tau polymerization: role of the amino terminus. *Biochemistry (Mosc).* **42**, 2252–2257.

Gamblin T.C., Chen F., Zambrano A. *et al.* (2003b) Caspase cleavage of tau: linking amyloid and neurofibrillary tangles in Alzheimer's disease. *Proc. Natl Acad. Sci. USA* **100**, 10032–10037.

Garcia-Sierra F., Wischik C.M., Harrington C.R., Luna-Munoz J., Mena R. (2001) Accumulation of C-terminally truncated tau protein associated with vulnerability of the perforant pathway in early stages of neurofibrillary pathology in Alzheimer's disease. *J. Chem. Neuroanat.* **22**, 65–77.

Garcia-Sierra F., Ghoshal N., Quinn B., Berry R.W., Binder L.I. (2003) Conformational changes and truncation of tau protein during tangle evolution in Alzheimer's disease. *J. Alzheimers Dis.* **5**, 65–77.

Ghoshal N., Garcia-Sierra F., Fu Y. *et al.* (2001) Tau-66: evidence for a novel tau conformation in Alzheimer's disease. *J. Neurochem.* **77**, 1372–1385.

Gingrich J.R. & Roder J. (1998) Inducible gene expression in the nervous system of transgenic mice. *Annu. Rev. Neurosci.* **21**, 377–405.

Goedert M., Jakes R., Vanmechelen E. (1995) Monoclonal antibody AT8 recognises tau protein phosphorylated at both serine 202 and threonine 205. *Neurosci. Lett.* **189**, 167–169.

Gong C.X., Liu F., Wu G. *et al.* (2004) Dephosphorylation of microtubule-associated protein tau by protein phosphatase 5. *J. Neurochem.* **88**, 298–310.

Goode B.L., Denis P.E., Panda D. *et al.* (1997) Functional interactions between the proline-rich and repeat regions of tau enhance microtubule binding and assembly. *Mol. Biol. Cell* **8**, 353–365.

Grundke-Iqbal I., Iqbal K., Tung Y.C., Quinlan M., Wisniewski H.M., Binder L.I. (1986) Abnormal phosphorylation of the microtubule-associated protein tau (tau) in Alzheimer cytoskeletal pathology. *Proc. Natl Acad. Sci. USA* **83**, 4913–4917.

Guillozet-Bongaarts A.L., Garcia-Sierra F., Reynolds M.R. *et al.* (2005) Tau truncation during neurofibrillary tangle evolution in Alzheimer's disease. *Neurobiol. Aging* **26**, 1015–1022.

Guillozet-Bongaarts A.L., Cahill M.E., Cryns V.L., Reynolds M.R., Berry R.W., Binder L.I. (2006) Pseudophosphorylation of tau at serine 422 inhibits caspase cleavage: in vitro evidence and implications for tangle formation in vivo. *J. Neurochem.* **97**, 1005–1014.

Gustke N., Trinczek B., Biernat J., Mandelkow E.M., Mandelkow E. (1994) Domains of tau protein and interactions with microtubules. *Biochemistry (Mosc).* **33**, 9511–9522.

Iqbal K., Alonso A.C., Gong C.X. *et al.* (1998) Mechanisms of neurofibrillary degeneration and the formation of neurofibrillary tangles. *J. Neural Transm. Suppl.* **53**, 169–180.

Ishiguro K., Shiratsuchi A., Sato S. *et al.* (1993) Glycogen synthase kinase 3 beta is identical to tau protein kinase I generating several epitopes of paired helical filaments. *FEBS Lett.* **325**, 167–172.

King M.E., Ahuja V., Binder L.I., Kuret J. (1999) Ligand-dependent tau filament formation: implications for Alzheimer's disease progression. *Biochemistry (Mosc).* **38**, 14851–14859.

Lucas J.J., Hernández F., Gómez-Ramos P., Moráo M.A., Hen R., Arila J. (2001) Decreased nuclear β-catenin, tau hyperphosphorylation and neurodegeneration in GSK-3β conditioned transgenic mice. *The EMBO Journal* **20**, 27–39.

Luna-Munoz J., Garcia-Sierra F., Falcon V., Menendez I., Chavez-Macias L., Mena R. (2005) Regional conformational change involving phosphorylation of tau protein at the Thr231, precedes the structural change detected by Alz-50 antibody in Alzheimer's disease. *J. Alzheimers Dis.* **8**, 29–41.

Matsui T., Ramasamy K., Ingelsson M. *et al.* (2006) Coordinated expression of caspase 8, 3 and 7 mRNA in temporal cortex of Alzheimer disease: relationship to formic acid extractable abeta42 levels. *J. Neuropathol. Exp. Neurol.* **65**, 508–515.

Mena R., Edwards P.C., Harrington C.R., Mukaetova-Ladinska E.B., Wischik C.M. (1996) Staging the pathological assembly of truncated tau protein into paired helical filaments in Alzheimer's disease. *Acta Neuropathol. (Berl).* **91**, 633–641.

Otvos L. Jr., Feiner L., Lang E., Szendrei G.I., Goedert M., Lee V.M. (1994) Monoclonal antibody PHF-1 recognizes tau protein phosphorylated at serine residues 396 and 404. *J. Neurosci. Res.* **39**, 669–673.

Raina A.K., Hochman A., Zhu X. *et al.* (2001) Abortive apoptosis in Alzheimer's disease. *Acta Neuropathol. (Berl).* **101**, 305–310.

Raina A.K., Zhu X., Shimohama S., Perry G., Smith M.A. (2003) Tipping the apoptotic balance in Alzheimer's disease: the abortosis concept. *Cell Biochem. Biophys.* **39**, 249–255.

Rissman R.A., Poon W.W., Blurton-Jones M. *et al.* (2004) Caspase-cleavage of tau is an early event in Alzheimer disease tangle pathology. *J. Clin. Invest.* **114**, 121–130.

Rohn T.T., Head E., Nesse W.H., Cotman C.W., Cribbs D.H. (2001) Activation of caspase-8 in the Alzheimer's disease brain. *Neurobiol. Dis.* **8**, 1006–1016.

Rohn T.T., Rissman R.A., Davis M.C., Kim Y.E., Cotman C.W., Head E. (2002) Caspase-9 activation and caspase cleavage of tau in the Alzheimer's disease brain. *Neurobiol. Dis.* **11**, 341–354.

Roth M., Tym E., Mountjoy C.Q. *et al.* (1986) CAMDEX. A standardised instrument for the diagnosis of mental disorder in the elderly with special reference to the early detection of dementia. *Br. J. Psychiatry* **149**, 698–709.

Timm T., Matenia D., Li X.Y., Griesshaber B., Mandelkow E.M. (2006) Signaling from MARK to tau: regulation, cytoskeletal crosstalk, and pathological phosphorylation. *Neurodegener. Dis.* **3**, 207–217.

Van Hoesen G.W. & Hyman B.T. (1990) Hippocampal formation: anatomy and the patterns of pathology in Alzheimer's disease. *Prog. Brain Res.* **83**, 445–457.

Van Hoesen G.W., Hyman B.T., Damasio A.R. (1991) Entorhinal cortex pathology in Alzheimer's disease. *Hippocampus* **1**, 1–8.

Yu J.Z. & Rasenick M.M. (2006) Tau associates with actin in differentiating PC12 cells. *FASEB J.* **20**, 1452–1461.

Zhu X., Raina A.K., Perry G., Smith M.A. (2004) Alzheimer's disease: the two-hit hypothesis. *Lancet Neurol.* **3**, 219–226.

Zhu X., Raina A.K., Perry G., Smith M.A. (2006) Apoptosis in Alzheimer disease: a mathematical improbability. *Curr. Alzheimer Res.* **3**, 393–396.

